

Characterization of diffusion complexity in prostate tissue with a stretched biexponential model

Roger M. Bourne¹ and Matt G. Hall²

¹University of Sydney, Sydney, NSW, Australia, ²University College London, London, United Kingdom

Target Audience Biophysical modellers, diffusion MRI researchers, and cancer imaging researchers.

Purpose When prostate DWI signal attenuation is measured over a large range of b -values the behavior is non-monoexponential – consistent with the microscopic complexity of tissue structure. Development of measurement and analysis methods that extract more tissue structure information than the monoexponential ADC model can be expected to provide an evidence base for improvement of DWI methods for clinical prostate cancer imaging. A recent comparison of monoexponential, biexponential, kurtosis, and stretched exponential models applied to prostate data shows the biexponential and kurtosis models have much higher information content and thus prediction accuracy than the stretched and monoexponential models. As maximum b -value increases above $\sim 2000 \mu\text{m}^2/\text{ms}$ the biexponential becomes increasingly superior to the kurtosis model¹. In this study we explore a further development of the conventional biexponential model by adding a stretching factor to the lower diffusivity component.

Methods MRI Acquisition. A formalin fixed radical prostatectomy specimen was imaged in a 9.4T Bruker Biospec scanner² using a PGSE sequence with diffusion times $\Delta = 20, 40, 80\text{ms}$ and $\delta = 5\text{ms}$. The diffusion gradients were placed along the three imaging coordinate axes with 17 log-spaced b -values from 0.017 to 10.23 $\text{ms}/\mu\text{m}^2$, FOV 45x45mm, matrix 32x32, TE 28, 48, 88ms, TR 2200ms, giving $\text{SNR}_{b=0} = 269, 114, 40$ for $\Delta = 20, 40, 80\text{ms}$ respectively.

Diffusion Models. We fitted two diffusion models to each voxel and gradient direction using a nonlinear least squares method in Matlab:

$$\text{Biexponential (BIEX): } S = S_{01}e^{-bD_1} + S_{02}e^{-bD_2}$$

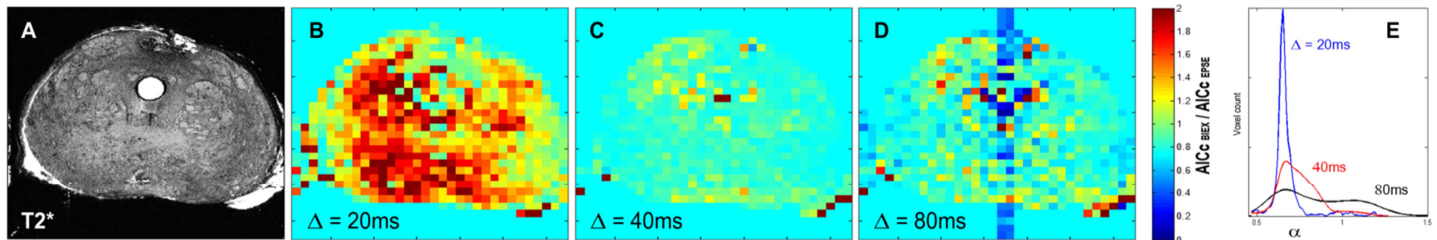
$$\text{Exponential-stretched exponential (EXSE): } S = S_{01}e^{-bD_1} + S_{02}e^{-(bD_2)^\alpha}$$

Model Testing For each voxel we used a leave-one-out (LOO) method to perform 17 fits to measurements at 16 b -values. For each fit we stored the parameter values and the sum of squared errors, and the average ($n = 17$) of these was taken as the parameter value and fitting error (SSE) for the voxel. For each of the 17 fits for each voxel we used the fitted parameters to estimate the value of the omitted measurement. The squared estimate errors were summed to produce a total model prediction error (LOO-SSE). From the SSE we calculated the Akaike Information Criterion with overfitting compensation (AICc):

$$\text{AICc} = \left(\frac{\text{SSE}}{\sigma^2}\right) + \frac{2np}{(n-p-1)}$$

where σ is the noise standard deviation measured from a pair of un-weighted reference images, n is the number of fitted parameters (4 and 5 for BIEX and EXSE, respectively) and $p = 16$ is the number of measurements¹.

Results There was a strong linear correlation between AICc and LOO-SSE indicating that AICc was a reliable estimator of model prediction performance. Fig. 1 shows typical results for relative model performance expressed as the ratio of AICc (BIEX/EXSE) at the three diffusion times $\Delta = 20, 40, 80\text{ms}$. A ratio greater than one indicates better prediction performance by the EXSE model. The EXSE model performed better than BIEX in the majority of voxels with the difference increasing as diffusion time decreased. The BIEX and EXSE models returned similar mean values for D_1 ($1.1 \mu\text{m}^2/\text{ms}$ at all Δ). At smaller diffusion times, D_2 was higher for EXSE (0.21, 0.16, 0.11 $\mu\text{m}^2/\text{ms}$, $\Delta = 20, 40, 80\text{ms}$) than for BIEX (0.12, 0.11, 0.09 $\mu\text{m}^2/\text{ms}$). The mean α values were 0.64, 0.71, 0.81 for $\Delta = 20, 40, 80\text{ms}$.



Discussion The superior information content and prediction performance of the EXSE over the BIEX model at short diffusion time is consistent with the presence of a complex diffusion environment experienced by the “slow” component of the conventional biexponential model. This result is indicative of environmental complexity at shorter length scales which is then averaged out as the diffusion time increases and the length scale of diffusion increases. In this limit the “slow” component is well-described by a monoexponential and the stretching exponent (α) provides no extra information. The value of the stretching exponent is linked to the complexity of the environment -- the greater the difference from one, the more complex the environment^{3,4}. The histogram of exponents shows this peak shrinking at longer diffusion times and a broader peak around $\alpha = 1$ emerging, possibly indicating the presence of two slow sub-components.

Conclusion The EXSE model has a higher information content than the BIEX model at shorter diffusion times. At the limit of short diffusion times we would expect diffusion to be free. At very long diffusion times we would expect a long-time limit in which diffusion is well-described by an effective diffusion constant. In between these regimes there exists a region in which diffusion is transitioning from one to the other. The current results suggest that this is what is being probed with a 20ms diffusion time. Under these circumstances we expect to observe a different form of diffusion with a different time dependence – this is known as anomalous diffusion³. The theory of anomalous diffusion predicts the diffusion-weighted signal decay should take the form of a Mittag-Leffler function⁴, of which the stretched exponential is a special case. In future it would be interesting to apply the Mittag-Leffler model to this data.

References

1. Bourne, R., et al., *Information theoretic ranking of four models of diffusion attenuation in fresh and fixed prostate tissue ex vivo*. Magnetic Resonance in Medicine, 2013: p. (In press. Accepted 15 Oct 2013).
2. Bourne, R., et al., *Effect of formalin fixation on biexponential modeling of diffusion decay in prostate tissue*. Magnetic Resonance in Medicine, 2013. **70**(4): p. 1160-1166.
3. Hall, M.G. and T.R. Barrick, *From diffusion-weighted MRI to anomalous diffusion imaging*. Magnetic Resonance in Medicine, 2008. **59**(3): p. 447-455.
4. Zhou, X.J., et al., *Studies of Anomalous Diffusion in the Human Brain Using Fractional Order Calculus*. Magnetic Resonance in Medicine, 2010. **63**(3): p. 562-569.